Cell Death and Differentiation (2016) 23, 2031–2041
 1350-9047/16
www.nature.com/cdd

The oncolytic compound LTX-401 targets the Golgi apparatus

This article has been corrected since Online Publication and a Corrigendum has also been Published

Heng Zhou[1,2,3,4,5], Allan Sauvat[1,2,3,4], Lígia C Gomes-da-Silva[1,2,3,4,6], Sylvère Durand[1,2,3,4], Sabrina Forveille[1,2,3,4], Kristina Iribarren[1,2,3,4], Takahiro Yamazaki[5,7,8,9], Sylvie Souquere[10], Lucillia Bezu[1,2,3,4,5], Kevin Müller[1,2,3,4,5], Marion Leduc[1,2,3,4], Peng Liu[1,2,3,4,5], Liwei Zhao[1,2,3,4,5], Aurélien Marabelle[8], Laurence Zitvogel[5,7,8,9], Øystein Rekdal[11,12], Oliver Kepp*[,1,2,3,4] and Guido Kroemer*[,1,2,3,4,13,14]

LTX-401 is an oncolytic amino acid derivative with potential immunogenic properties. Here, we demonstrate that LTX-401 selectively destroys the structure of the Golgi apparatus, as determined by means of ultrastructural analyses and fluorescence microscopic observation of cells expressing Golgi-targeted GFP reporters. Subcellular fractionation followed by mass spectrometric detection revealed that LTX-401 selectively enriched in the Golgi rather than in mitochondria or in the cytosol. The Golgi-dissociating agent Brefeldin A (BFA) reduced cell killing by LTX-401 as it partially inhibited LTX-401-induced mitochondrial release of cytochrome *c* and the activation of BAX. The cytotoxic effect of LTX-401 was attenuated by the double knockout of BAX and BAK, as well as the mitophagy-enforced depletion of mitochondria, yet was refractory to caspase inhibition. LTX-401 induced all major hallmarks of immunogenic cell death detectable with biosensor cell lines including calreticulin exposure, ATP release, HMGB1 exodus and a type-1 interferon response. Moreover, LTX-401-treated tumors manifested a strong lymphoid infiltration. Altogether these results support the contention that LTX-401 can stimulate immunogenic cell death through a pathway in which Golgi-localized LTX-401 operates upstream of mitochondrial membrane permeabilization.
Cell Death and Differentiation (2016) **23,** 2031–2041; doi:10.1038/cdd.2016.86; published online 2 September 2016

LTX-401, formerly known as BAA-1, is an amphipathic β(2,2)-amino acid derivative that is being synthesized as a potential anticancer agent. Owing to its amphipathic nature, LTX-401 may affect the integrity of biological membranes.[1,2] With respect to this property, it resembles antimicrobial peptides that usually contain cationic amino acid residues interspersed with lipophilic ones to create an amphipathic, potentially membrane-permeabilizing structure as exemplified for LTX-315.[3,4]

LTX-315 is being developed for the local treatment of superficial human cancers based on the observations that it causes potent cytotoxic effects and that it might stimulate a local immune response that may prolong its antineoplastic action over time.[5–7] This latter property makes LTX-315 an interesting lead compound, especially in view of its capacity to reverse the resistance of cancers to immune checkpoint blockade with anti-CTLA4 antibodies in preclinical models.[6] LTX-315 has the capacity of causing a necrotic cell death (i.e., cell death without caspase activation and without morphological features of apoptosis such as nuclear fragmentation) that is partially relying on mitochondrial membrane permeabilization by this oncolytic peptide,[4] which actually redistributes specifically towards the mitochondrial compartment.[8] LTX-315 has also been found to stimulate a series of alterations in cancer cells that give rise to immunogenic cell death (ICD), that is, a type of cell death that elicits a potent anticancer immune response.[9] Accordingly, LTX-315 triggers the exposure or release of several danger-associated molecular patterns (DAMPs) associated with ICD, namely the translocation of calreticulin (CALR) from the lumen of the endoplasmic reticulum to the cell surface; the release of ATP from cytoplasmic storage sites into the extracellular space; the exodus of high mobility group box 1 (HMGB1) from the nucleus to the extracellular milieu; and a type-1 interferon response.[5,10] Through the combination of these DAMPs, LTX-315-induced cell death can alert innate immune effectors including dendritic cells, hence starting a cascade of

[1]Metabolomics and Cell Biology Platforms, Gustave Roussy Comprehensive Cancer Institute, Villejuif 94805, France; [2]Equipe 11 labellisée Ligue contre le Cancer, Centre de Recherche des Cordeliers, INSERM U1138, Paris 75006, France; [3]Université Paris Descartes, Sorbonne Paris Cité, Paris 75006, France; [4]Université Pierre et Marie Curie, 15 rue de l'Ecole de Médecine, Paris 75006, France; [5]University of Paris Sud XI, Le Kremlin-Bicêtre 94276, France; [6]Chemistry Department, University of Coimbra, Coimbra 3004-535, Portugal; [7]Department of Immuno-Oncology, Institut de Cancérologie Gustave Roussy Cancer Campus, 114 rue Edouard Vaillant, Villejuif 94805, France; [8]Institut National de la Santé et de la Recherche Medicale (INSERM), U1015, Villejuif, France; [9]Center of Clinical Investigations in Biotherapies of Cancer (CICBT) 507, Villejuif, France; [10]Gustave Roussy Comprehensive Cancer Center, Villejuif, France CNRS, UMR9196, Villejuif, France; [11]Lytix Biopharma AS, Oslo 0349, Norway; [12]Institute of Medical Biology, University of Tromsø, 9037 Tromsø, Norway; [13]Pôle de Biologie, Hôpital Européen Georges Pompidou, AP-HP, Paris 75015, France and [14]Karolinska Institute, Department of Women's and Children's Health, Karolinska University Hospital, Stockholm 17176, Sweden
*Corresponding author: G Kroemer or O Kepp, U1138, INSERM, Centre de Recherche les Cordeliers, 15 rue de l'ecole de medicine, Paris F-75006, France. Tel: +33 1 44 27 76 67; Fax: +33 1 44 27 76 74; E-mail: kroemer@orange.fr or captain.olsen@gmail.com

Abbreviations: ATP, adenosine triphosphate; BFA, brefeldin A; CALR, calreticulin; CCCP, *m*-chlorophenylhydrazone; COPI, coat protein I; CYTC, cytochrome *c*; DAMP, danger-associated molecular pattern; DAPI, 4',6-diamidino-2-phenylindole; $DiOC_6(3)$, 3,3 dihexyloxacarbocyanine; DKO, double knockout; GALT1, galactose-1-phosphate uridylyltransferase; GFP, green fluorescent protein; ICD, immunogenic cell death; HMGB1, high mobility group box 1; MEF, mouse embryonic fibroblast; Z-VAD-fmk, *N*-benzyloxycarbonyl-V al-Ala-Asp-fluoromethylketone

Received 27.6.16; revised 19.7.16; accepted 20.7.16; Edited by H-U Simon; published online 2 September 2016

molecular events that culminates in a strong cellular immune response against tumor-associated antigens.[5,7]

LTX-315 is a peptide encompassing nine amino acids residues, spurring interest in alternative compounds like LTX-401 that might share similar pharmacological properties. Indeed, LTX-401 has been shown to exert strong anticancer effects in a mouse model of melanoma, in which it stimulates infiltration of the tumor by T lymphocytes.[10] Reportedly, LTX-401 exerts potent effects on the plasma membrane, causing its permeabilization.[1] However, LTX-401 may also affect the interior of the cell, as exemplified by the observation that it causes a strong cytoplasmic vacuolization accompanied by loss of the acidic pH of lysosomes.[2]

Given the scarcity of information on the molecular mode of action of LTX-401, we decided to determine the mechanistic basis of its anticancer action. Here, we report that LTX-401 selectively enriches in the Golgi apparatus, disrupts its structure and ignites a lethal signaling pathway that might be initiated at the level of this organelle, later causing caspase-independent, but partially mitochondrion-dependent, cell death. In addition, we found that LTX-401 elicited all known hallmarks of ICD.

Results and Discussion

LTX-401 disrupts the morphology of the Golgi apparatus. Incubation of human osteosarcoma U2OS cells with LTX-401 induced the accumulation of electron-dense material in the Golgi (especially at lower concentrations) that was accompanied by its structural disruption and prominent cytoplasmic vacuolization (especially at higher LTX-401 doses). Although it was not possible to determine the organellar origin of each vacuole, Golgi-derived structures appeared to play a prominent role in this vacuolization process (Figure 1a). In accord with the interpretation of these transmission electron microscopic data, immunofluorescence staining of the Golgi marker galactose-1-phosphate uridylyltransferase (GALT1) revealed that increasing concentrations of LTX-401 caused a progressive dissociation of the Golgi. Instead of the normal perinuclear accumulation of GALT1 in one pole, the staining pattern turned diffuse, confirming the disruption of the normal structure of the Golgi (Figures 1b and c). U2OS cells stably expressing a GALT1-GFP fusion protein as a biosensor for measuring Golgi integrity also revealed destruction of the organelle upon treatment with LTX-401 (Figure 2a). These effects were much more pronounced than with the oncolytic peptide LTX-315. Morphometric analyses indicated that the diminution of identifiable GALT1-GFP dots (that indicate the presence of an intact Golgi) was reduced at relatively low LTX-401 doses that had not yet affected nuclear and cellular morphology, contrasting with LTX-315 that compromised cellular health even at doses that had no significant effect on GALT1-GFP dots (Figures 2b and c). Time-lapse videomicroscopy indicated that LTX-401 (but not LTX-315) rapidly fragmented the sole Golgi-associated GALT1-GFP dot found in normal cells into several smaller structures before their complete dissipation in the cytoplasm (Figure 2d), confirming the quantitative result shown above (Figure 2a). Altogether these results support the contention that LTX-401 has the capacity to destroy the Golgi apparatus in otherwise intact cells, before their viability is loss.

Preferential subcellular distribution of LTX-401 into the Golgi apparatus. Intrigued by the aforementioned observation, we decided to determine the subcellular distribution of LTX-401 by means of mass spectrometry (Figures 3a and b). For this, we incubated cells with a subtoxic concentration of LTX-401, followed by their mechanical disruption and differential gradient centrifugation to obtain cytosolic, mitochondrial and Golgi-enriched fractions (Figure 3c), and determined the abundance of LTX-401 in each fraction. LTX-401 was preferentially enriched in the cytosolic and Golgi fractions, not in mitochondria (Figure 3c). This strongly contrasts with LTX-315 that preferentially enriches in the mitochondrial fraction,[8] not in the Golgi (Figure 3d). Altogether these results suggest that LTX-401 may disrupt the Golgi via a direct effect, upon reaching high local concentrations.

Brefeldin A inhibits LTX-401-induced cell killing. Brefeldin A (BFA) is a lactonic antibiotic that blocks protein transport from the endoplasmic reticulum to the Golgi by preventing formation of coat protein I (COPI)-mediated transport vesicles.[11] When added to cells, BFA and LTX-401 induced a similar dissociation of GALT1-GFP dots (Figure 4a). Intriguingly, BFA also reduced the cytotoxic activity of LTX-401, hence augmenting the proportion of cells that survived treatment with the oncolytic compound (Figure 4b) while the pan-caspase inhibitor Z-VAD-fmk failed to do so (Figure 4c). These results indicate that prophylactic dissociation of the Golgi by BFA, a manipulation that has neither an impact on staurosporin-induced apoptosis (Figures 4b and c) nor on LTX-315-mediated killing (not shown), can reduce the cytotoxic potential of LTX-401.

BFA reduces LTX-401-induced mitochondrial permeabilization. Although LTX-401 does not primarily enrich in mitochondria, it does cause signs of mitochondrial membrane permeabilization, as detectable in U2OS biosensor cells stably expressing an SMAC-GFP fusion protein that usually is located in the mitochondrial intermembrane space.[12] Upon treatment with LTX-401, SMAC-GFP redistributed from its punctate (mitochondrion-associated) to a diffuse cytosolic pattern, especially when LTX-401 was used at cytotoxic concentrations ($>10\,\mu$g/ml). Importantly, this effect of LTX-401 was inhibited when BFA was added to the cells as well (Figures 5a and b). Very similar results were obtained when cytochrome *c* (CYTC), another mitochondrial intermembrane protein, was detected by immunofluorescence staining of fixed and permeabilized cells. LTX-401 caused mitochondrial CYTC release, and BFA reduced this effect (Figures 5c and d). Altogether, these results suggest that BFA can interrupt the lethal cascade ignited by LTX-401 at the level (or upstream) of mitochondria, suggesting that the Golgi-related effects of BFA are the cause of subsequent mitochondrial alterations, not vice versa.

Contribution of mitochondria to LTX-401-mediated killing. Driven by the aforementioned considerations, we evaluated the possible contribution of mitochondrial

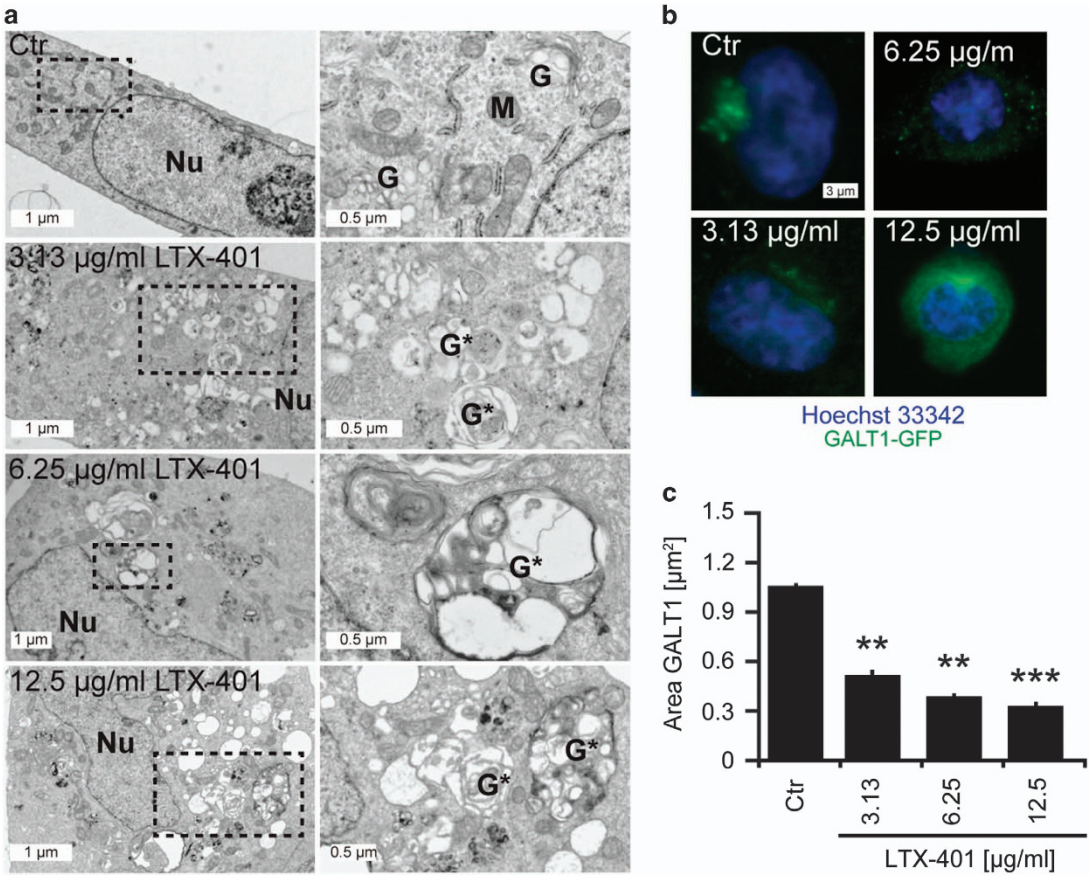

Figure 1 Ultrastructural characteristics of LTX-401-induced Golgi fragmentation. (**a**) Human osteosarcoma U2OS cells were either left untreated (control, Ctr) or treated with the indicated concentrations of LTX-401 for 6 h, fixed by glutaraldehyde, post-fixed with osmium tetroxide and finally analyzed by conventional transmission electron microscopy. Low-magnification micrographs on the left are enlarged in insets on the right side. Note the presence of electron-dense material in the Golgi and dilated Golgi in cells treated with 3.13 and 6.25; 12.5 μg/ml of LTX-401, respectively. (**b** and **c**) U2OS stably expressing the trans-Golgi marker GALT1-GFP were treated for 6 h with the indicated concentrations of LTX-401, followed by nuclear counterstain with Hoechst 33342 before microscopic analysis. Representative images are shown in (**b**). The decrease in GALT1-GFP+ signal was measured as an indication for Golgi fragmentation with increasing concentrations of LTX-401. M marks mitochondria, G intact Golgi and G* dilated/fragmented Golgi structures. Scale bars equal 1 and 0.5 μm, respectively. Asterisks indicate significant differences (unpaired Student *t*-test) with respect to untreated controls. $^{*}P<0.05$; $^{**}P<0.01$; $^{***}P<0.001$

membrane permeabilization to LTX-401-mediated cytotoxicity using two approaches, namely (i) the double knockout (DKO) of the two major pro-apoptotic multidomain proteins of the Bcl-2 family, BAX and BAK[13] and (ii) the Parkin-driven mitophagy-enforced removal of mitochondria from otherwise intact cells.[14] Mouse embryonic fibroblasts (MEFs) as well as human colon carcinoma HCT116 cells subjected to the DKO of BAX and BAK[13,15] were partially resistant to LTX-401-mediated killing, meaning that the fraction of cells that manifested the dissipation of the mitochondrial inner transmembrane potential ($\Delta\Psi$m, measured with the cyanine dye $DiOC_6(3)$) and/or the loss of the plasma membrane integrity (measured with the vital dye 4′,6-diamidino-2-phenylindole, DAPI)[16] was reduced as compared with wild-type (WT) controls (Figures 6a and b). Despite the retardation of cell death, the Golgi fragmentation, which was induced by LTX-401 but not by LTX-315, was similarly observed in WT and DKO MEFs (Figure 6c). Moreover, mitochondrial depletion induced by stable transfection of U2OS cells with Parkin-mCherry (to increase their mitophagic potential) and long-term (48 h) treatment with the uncoupler carbonyl cyanide *m*-chlorophenylhydrazone (CCCP to induce mitophagy)[14] was able to confer partial protection against low cytotoxic doses of LTX-401 (12.5 μg/ml at 6 h and 6.25 μg/ml at 24 h) (Figures 6d and e). However, the depletion of mitochondria did not affect the LTX-401-driven Golgi fragmentation (Figure 6f). Altogether these results suggest that BAX/BAK and mitochondria contribute to LTX-401-induced cell killing, at least when the concentration of the compound is limiting and that Golgi fragmentation occurs as an upstream event that is not affected by BAX/BAK knockout or mitochondrial depletion.

LTX-401 induces signs of ICD. LTX-401 has previously been shown to stimulate the infiltration of locally injected B16F10 melanomas by $CD3^+$ T lymphocytes as it extends the survival of melanoma-bearing immunocompetent mice.[2] LTX-401 stimulated all major ICD hallmarks. Thus, U2OS cells stably expressing a calreticulin (CALR)-GFP fusion protein manifested a relocation of the protein from a

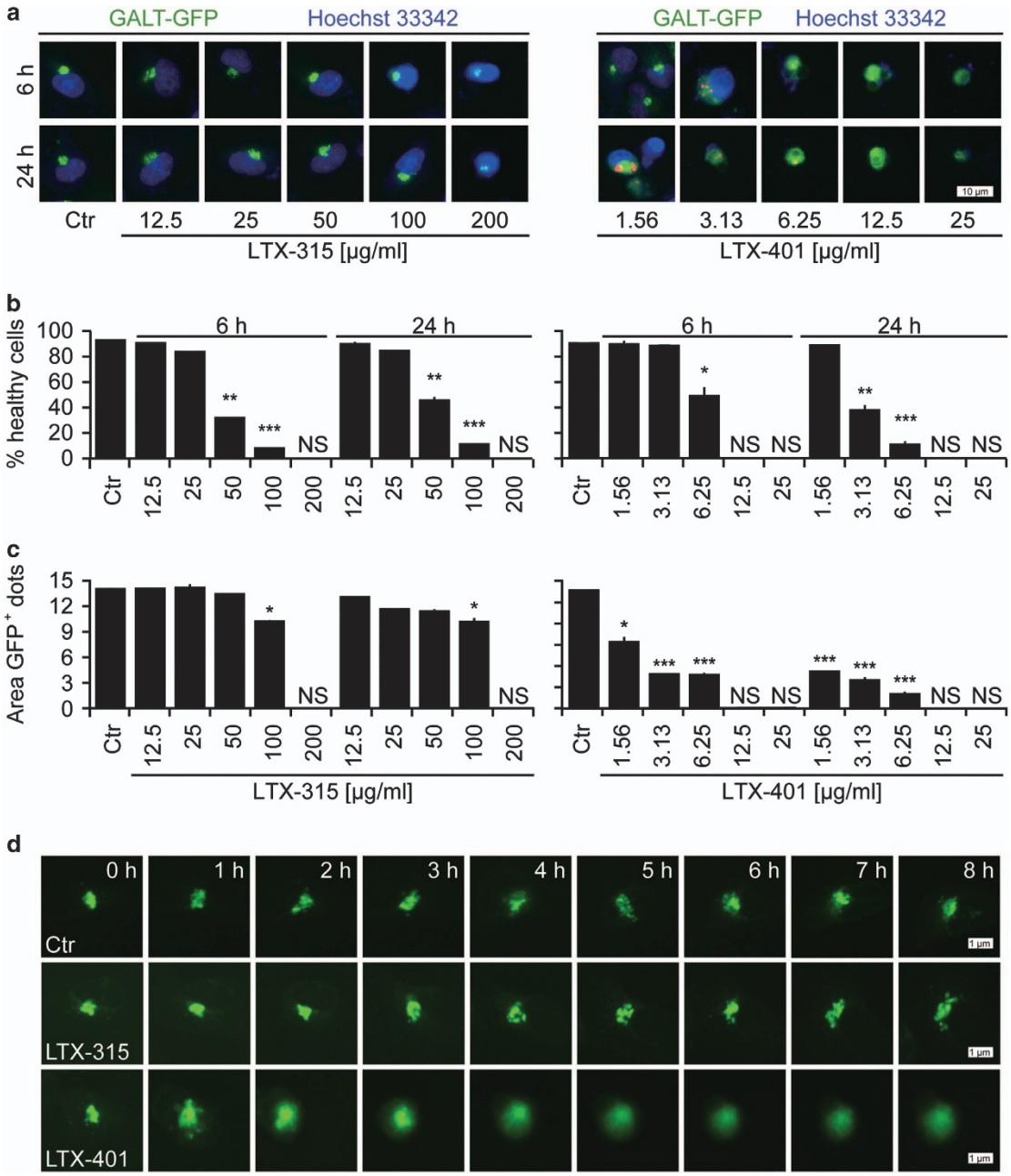

Figure 2 Differential effects on Golgi morphology induced by LTX-315 and LTX-401. (**a**) U2OS cells stably expressing GALT1-GFP were treated for the indicated period with the indicated concentrations, which covered the half maximum toxic effect, of LTX-315, or LTX-401, followed by fixation and nuclear counterstaining with the DNA intercalating dye Hoechst 33342. Representative images are shown in (**b**). Quantitative results (means ± S.D. of triplicates) for viability and Golgi fragmentation are shown in (**b** and **c**), respectively. In (**b**), the number of cells with normal nuclear morphology (not shrunken) is shown, while in (**c**), the average area of GALT1$^+$ Golgi structures per cell is displayed. (**d**) Time-lapse microscopy of U2OS cells stably expressing GALT1-GFP cells treated with 50 μg/ml LTX-315 or 6.25 μg/ml LTX-401 (that had similar effects on viability) showed the time-dependent fragmentation of the Golgi in one representative cell in response to LTX-401 but not to LTX-315. Asterisks indicate significant differences (unpaired Student *t*-test) with respect to untreated controls. *$P<0.05$; **$P<0.01$; ***$P<0.001$

perinuclear to a peripheral area of the cytoplasm when cultured in the presence of LTX-401 (Supplementary Figure S1). Moreover, LTX-401-treated cells exhibited immunofluorescence-detectable CALR exposure on the cell surface at a stage at which they were still viable and excluded the vital dye propidium iodide (PI) (Figures 7a and b). Similarly, LTX-401 caused the release of ATP from cells into the supernatant (Supplementary Figure S2) and triggered the exodus of nuclear HMGB1 into the cytoplasm and the extracellular space (Supplementary Figure S3). Finally, the supernatant of LTX-401-treated cells was able to stimulate the expression of the type-1 interferon response gene MX1 in a biosensor cell line (Figure 7c) as it induced the transcription of genes coding for type-1 interferons

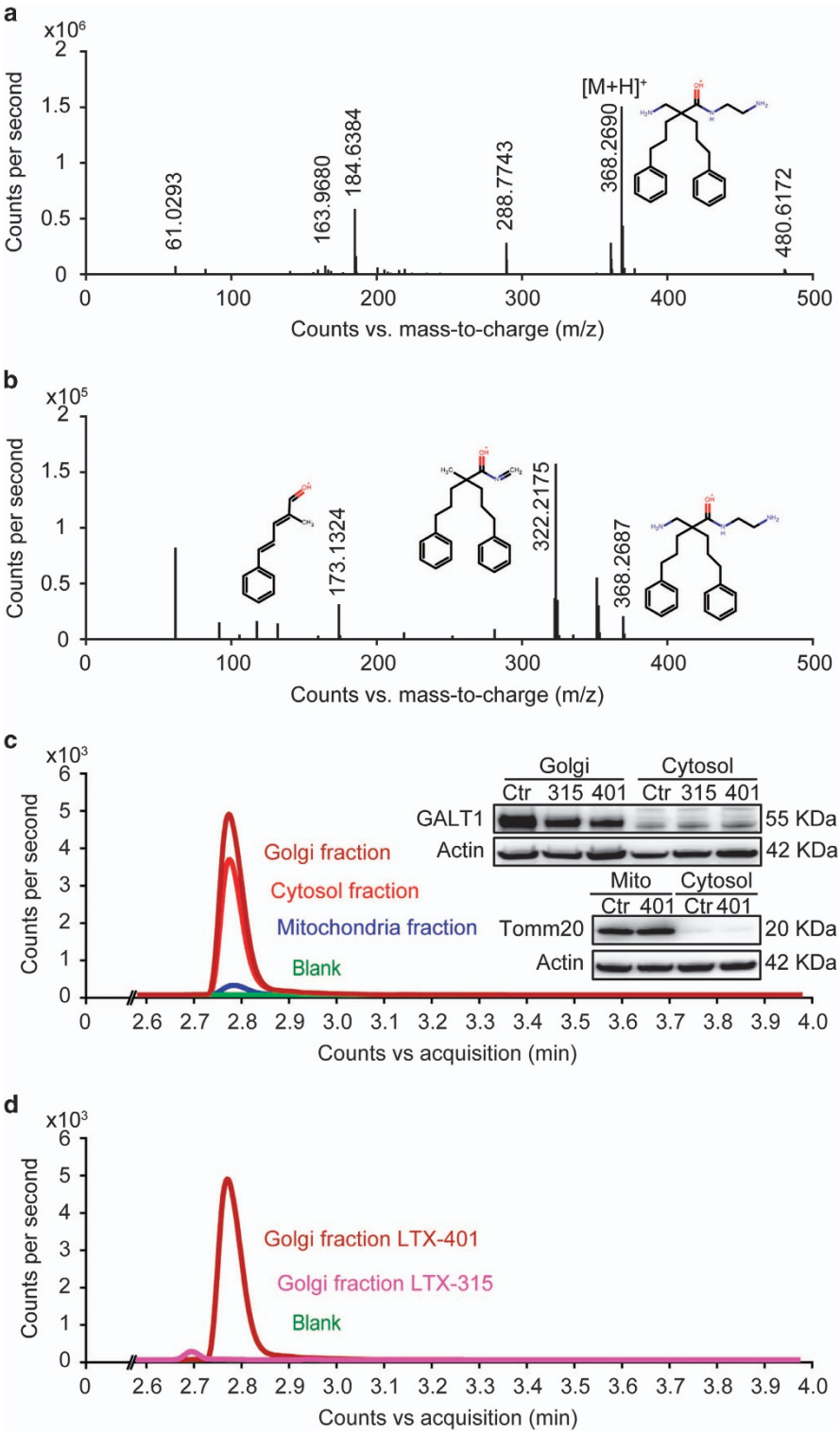

Figure 3 Mass spectrometric detection of LTX-401 enriched in the Golgi. (**a**) Full scan mass spectrum of LTX-401 ($C_{23}H_{33}N_3O$) revealed the structure of the amino acid derivative and its protonation level´ that yield in the signal used for quantification. (**b**) Selection and fragmentation of $[M+H]^+$. The hypothetical structure of the fragment are depicted. The fragment *m/z* 350.2582 corresponds to the loss of water and was excluded from the MRM transition due to lack of selectivity. (**c**) Subcellular fractionation of U2OS cells treated with 50 μg/ml of LTX-401 for 6 h yielded in cytoplasmic, Golgi- and mitochondria-enriched fractions that were tested for purity by immunobloting using mitochondria-specific TOMM20, and Golgi-specific GALT1 antibodies. Each fraction was analyzed and yielded in chromatographic peaks of LTX-401 in the Golgi, and cytosolic and mitochondrial fractions with different amplitudes. (**d**) Chromatography of Golgi-enriched fractions from subcellular fractions of U2OS cells treated with 6.25 μg/ml LTX-401 and 50 μg/ml LTX-315 for 6 h revealed that LTX-401 accumulates in Golgi fractions whereas LTX-315 does not

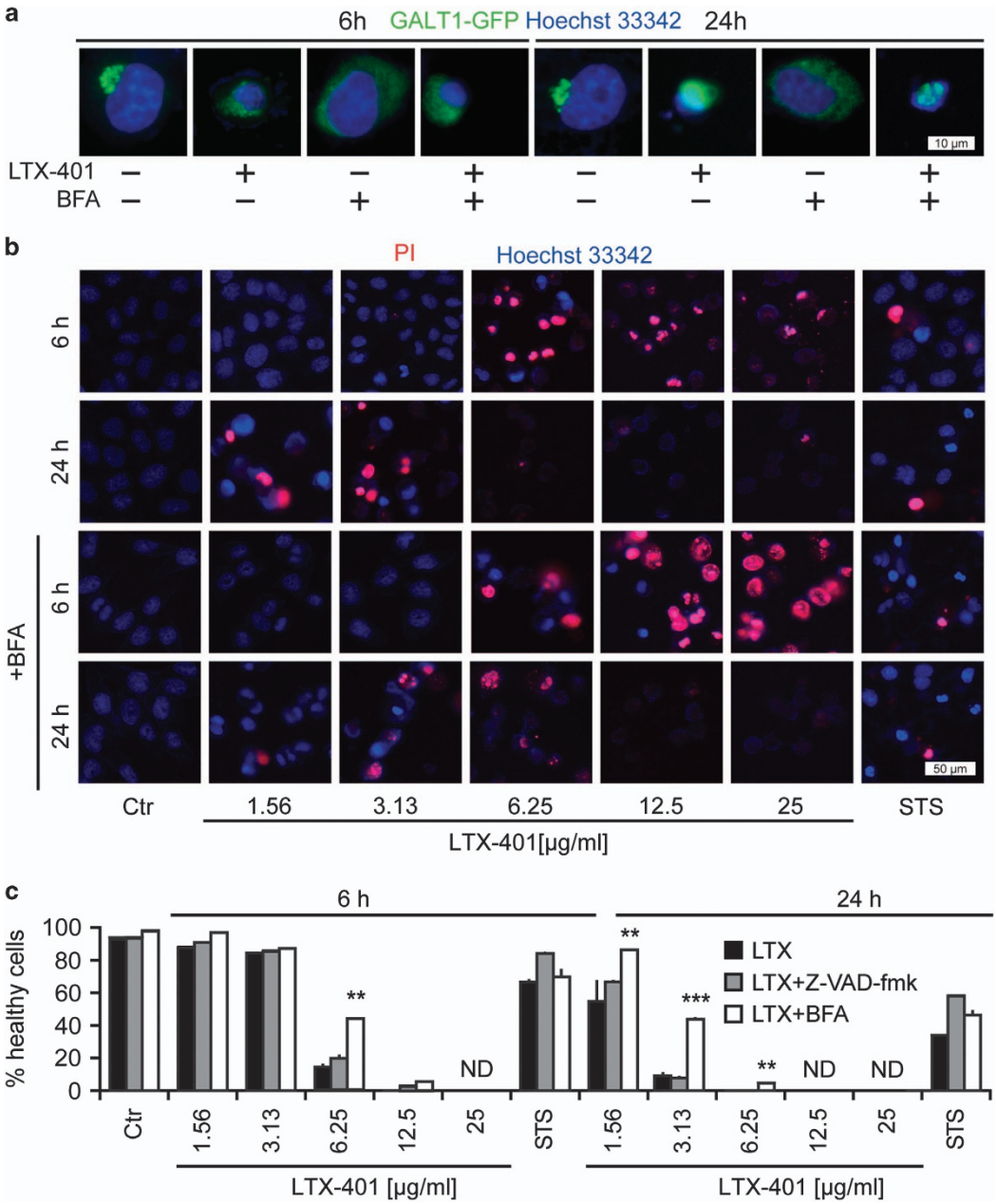

Figure 4 Brefeldin A inhibits LTX-401-induced cell killing. (**a**) U2OS cells stably expressing GALT1-GFP were treated with 6.25 μg/ml of LTX-401 in the presence or absence of the protein transport inhibitor brefeldin A (BFA; 10 μg/ml) for the indicated time. Dissociation of GALT1-GFP-marked Golgi structures in response to both LTX-401 and BFA are depicted in representative images in (**a**). U2OS cells were treated for 6 h with LTX-401 in the absence or presence of 10 μg/ml BFA, or the pan-caspase inhibitor Z-VAD-fmk (50 μM) followed by staining with the vital dye propidium iodide (PI) and the chromatin dye Hoechst 33342. Representative fluorescence microphotographs of LTX-401-treated cells in the presence and in the absence of BFA are depicted in (**b**), and quantitative results of all treatment conditions are shown in (**c**). Asterisks indicate significant differences (unpaired Student's *t*-test) in Hoechst^{dim} PI^{-} cell number with respect to untreated controls, for a given co-treatment. *$P<0.05$; **$P<0.01$; **$P<0.001$

(Figure 7d). When injected into subcutaneous MCA205 fibrosarcomas that had been established in mice, LTX-401 induced focal necrosis (Figures 8a and b) accompanied by dense lymphoid infiltration, especially at early time points (Figures 8c and d).

Concluding remarks. The results of this study suggest that LTX-401 kills cancer cells through a novel, unexpected pathway that involves its primary action on the Golgi apparatus, followed by the induction of an at least partially mitochondrion-dependent cell death pathway.

LTX-401 apparently targets the Golgi in the first place, as indicated by its capacity to rapidly destroy the structure of the organelle, as well as by the fact that LTX-401 preferentially redistributes into a subcellular fraction that is enriched in Golgi markers. With this respect, LTX-401 is rather distinct from LTX-315, which has been used as an internal control and which has no impact on the Golgi while it preferentially

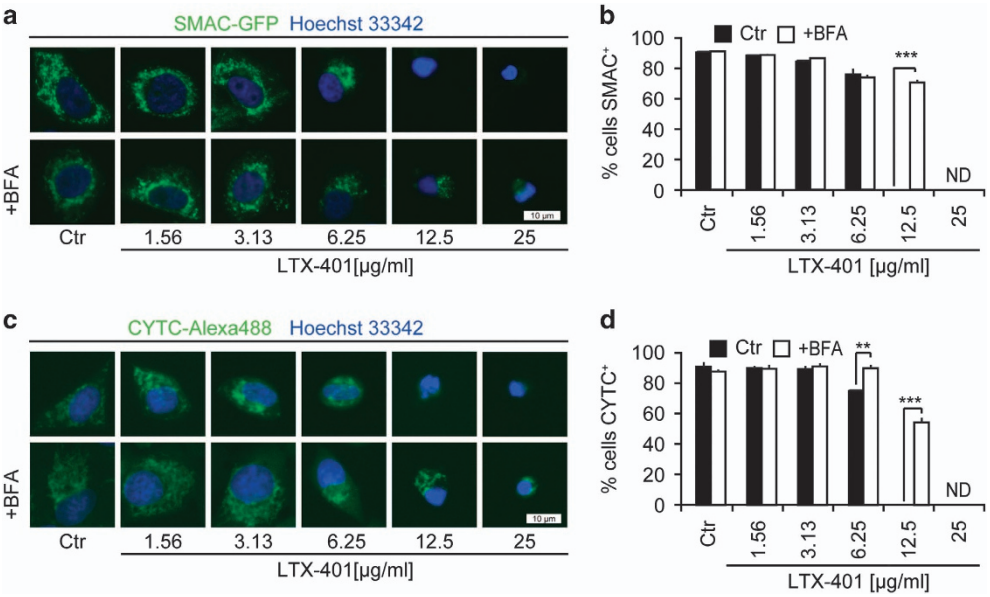

Figure 5 Mitochondrial outer membrane permeabilization induced by LTX-401. (**a** and **b**) U2OS cells stably transfected with SMAC-GFP fusion protein were cultured for 6 h in the presence or in the absence of 10 μM brefeldin A (BFA) with the indicated concentrations of LTX-401 and then counterstained with Hoechst 33342. Representative images of SMAC release are shown in (**a**) and quantitative results are depicted in (**b**). (**c** and **d**) The release of cytochrome *c* (CYTC) from U2OS cells cultured as in (**a**) and (**b**) was assessed by immunofluorescence detection of CYTC and counterstaining with Hoechst 33342. Representative pictures are shown in (**c**) and quantitative results are depicted in (**d**). Columns indicate means $\pm$ S.D. of triplicates. Asterisks indicate significant (unpaired Student's *t*-test) changes with respect to untreated controls (Ctr). $^{**}P<0.01$; $^{***}P<0.001$

redistributes into mitochondria. Thus, the initial mode of action of LTX-401 and LTX-315 is rather distinct. At this point, it is difficult to understand for which reason LTX-401 preferentially interacts with Golgi structures rather than with other cellular compartments. Whether this may be explained by the peculiar physicochemical properties of LTX-401 with respect to membrane interactions or interactions with specific proteins remains to be investigated in further detail.

Upon addition of LTX-401, cells lose the normal morphology of the Golgi apparatus within a short period (less than 1 h), as determined by time-lapse videomicroscopy. Similar to BFA, LTX-401 causes the dissipation of the initially normal Golgi structure (which usually is located in one perinuclear pole) towards a punctiform or diffuse distribution (as judged by fluorescence microscopy of Golgi markers) accompanied by general cytoplasmic vacuolization (as detectable by electron microscopy). However, in contrast to LTX-401, BFA is not particularly toxic to cells, in line with the observation that destruction/dissipation of the Golgi apparatus on its own is not sufficient to cause cell killing.[17,18] Rather, simultaneous treatment of cells with LTX-401 and BFA results in less cytotoxicity than treatment with LTX-401 alone, suggesting that the action of LTX-401 on the still intact Golgi ignites lethal signaling. What this signal might be remains to be clarified. Past studies have shown that Golgi can release ganglioside GD3,[19] BAX[20] and active caspase-2 (ref. 21) among other factors,[22] suggesting that Golgi can trigger cell death through a variety of distinct mechanisms.

While the initial lethal signal triggered by LTX-401 at the Golgi remains elusive, it appears clear that this organelle acts upstream of the mitochondrial checkpoint of cell death signaling. Thus, BFA can reduce the LTX-401-induced signs of mitochondrial membrane permeabilization (such as the release of the intermembrane proteins cytochrome *c* and SMAC), and DKO of the two pro-apoptotic multidomain proteins BAX and BAK (which both supposedly act on mitochondria) reduces LTX-401-induced killing. Moreover, mitophagy-enforced removal of mitochondria from the cells[8,14] reduces their susceptibility to LTX-401-mediated killing, yet does not reduce LTX-401-induced disruption of the Golgi. This observation again pleads in favor of the interpretation that mitochondria are secondary targets of LTX-401, downstream of its action on the Golgi. Downstream of mitochondria, then a variety of lethal signaling events (that can be partially inhibited by a combination of caspase inhibition by Z-VAD-fmk and RIP1 inhibition by necrostatin) come into action, as this is often observed,[23] in line with the increasing awareness that the clear-cut distinction between apoptotic and necroptotic degradation events is a didactic oversimplification.[24]

Similar to LTX-315,[5] LTX-401 triggers all biochemical hallmarks of ICD including ATP release, calreticulin exposure, nuclear HMGB1 exodus and the induction of a type-1 interferon response. These findings, which have been obtained *in vitro*, suggest that LTX-401 can stimulate the full spectrum of events required for (ATP-dependent) attraction of DC precursors into the tumor bed, the (calreticulin-dependent) transfer of tumor antigens from cancer cells to DC precursors, the (HMGB1-dependent) maturation of DC for optimal antigen presentation of tumor-associated antigens, and (the type-1 interferon-dependent) recruitment of T cells into the tumor bed. In line, with these notions, LTX-401 stimulates the

lymphoid infiltration of locally injected tumors in a preclinical mouse model.

In summary, LTX-401 kills cancer cells through a novel, Golgi-dependent pathway that culminates in ICD and may be therapeutically taken advantage of to stimulate anticancer immune responses.

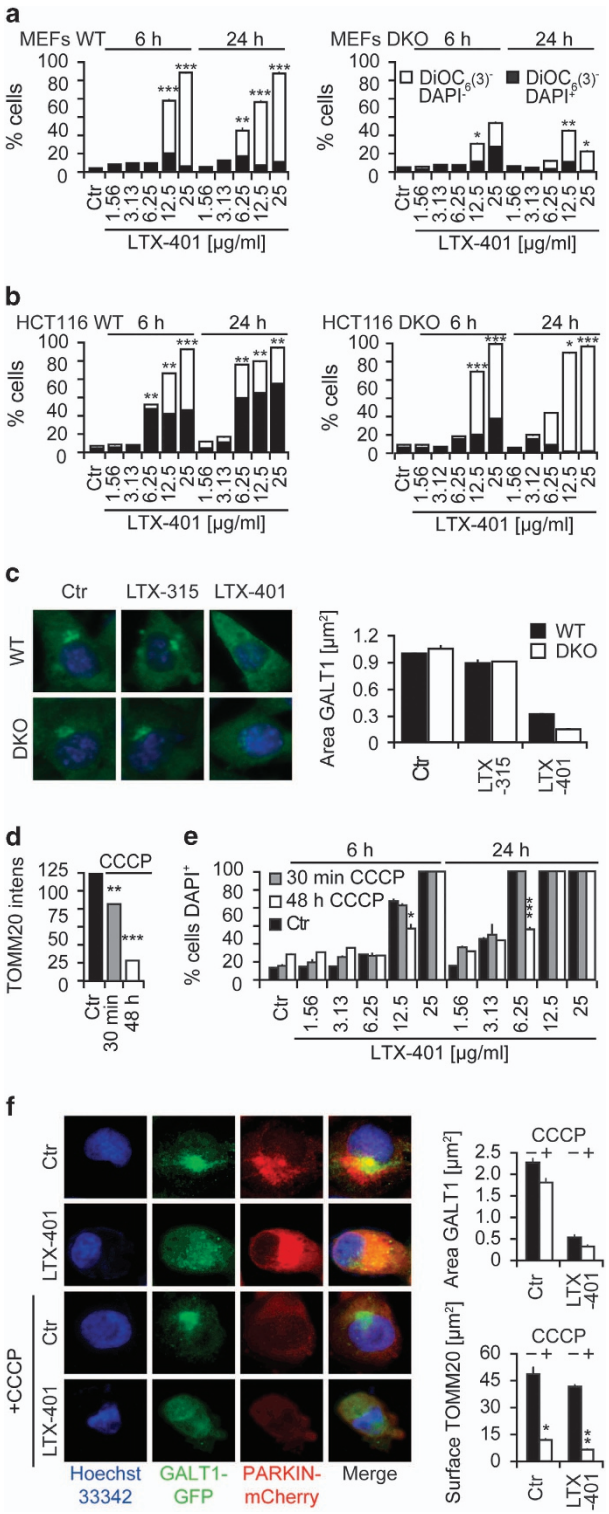

Materials and Methods

Cell culture and chemicals. Cell culture media and supplements were obtained from Gibco-Life Technologies (Carlsbad, CA, USA), plasticware was from Greiner Bio-One (Monroe, CA, USA), chemicals were obtained from Sigma Aldrich (St Louis, MO, USA), LTX-315 and LTX-401 were provided by Lytix Biopharma (Tromsø, Norway); CCCP was from R&D (Minneapolis, MN, USA). Chemical dyes including Hoechst 33342, DAPI, $DiOC_6(3)$, MitoTracker Green FM came from Life Technologies. Primary antibodies (cytochrome *c*, ab154476 and ab198583; TOMM20 ab78547) were obtained from Abcam (Cambridge, UK) and secondary AlexaFluor labeled antibodies came from Life Technologies. Human osteosarcoma U2OS WT or biosensors cells stably expressing GALT-GFP, SMAC-GFP, CALR-GFP or PARKIN-mCherry were cultured in Glutamax-containing DMEM medium supplemented with 10% fetal calf serum (FCS) and 10 mM HEPES buffer. U2OS that were genetically engineered as described[25] were cultured in DMEM GlutaMax supplemented with 10% FBS. In short, cells were stably transduced or transfected with cDNA vectors coding for the indicated fluorescent fusion proteins. Subsequently, stable expressing cells were selected by means of matched selection antibiotics and clones were obtained by single cell sorting using a FACS DIVA (Becton Dickinson, Franklin Lakes, NJ, USA). Human colorectal carcinoma HCT116 WT and $BAX^{-/-}$,$BAK^{-/-}$ DKO cells were cultured in Glutamax-containing DMEM medium supplemented with 10% FCS, and non-essential amino acids. MEF WT and $Bax^{-/-}$,$Bak^{-/-}$ DKO cells were cultured in Glutamax-containing RPMI medium supplemented with 10% FCS, and 10 mM HEPES buffer. All cell cultures were kept at 37 °C in a humidified incubator under 5% CO_2 atmosphere.

High-throughput assessment of mitochondrial PARKIN translocation, SMAC release Golgi fragmentation and calreticulin exposure. 5×10^3 U2OS cells stably expressing PARKIN-RFP, SMAC-GFP, GALT-GFP or CALR-GFP were seeded into black 96-well imaging plates (Greiner Bio-One) and allowed to adapt for 24 h. Thereafter the cells were treated with the indicated agents and respective controls and incubated for additional 6 or 24 h before fixation in 3.7% (w/v) paraformaldehyde in PBS supplemented with 1 μM Hoechst 33342 for 20 min. Upon fixation, PFA was substituted with PBS and a minimum of four view fields per well were acquired by means of an ImageXpress micro XL automated bioimager (Molecular Devices, Sunnyvale, CA, USA) equipped with a PlanApo 20X/0.75 NA objective (Nikon Tokyo, Japan). For some of the assays cells were stained with 200 nM MitoTracker green (Life Technologies) before imaging.

Figure 6 The role of mitochondria in LTX-401-mediated killing downstream of the Golgi. (**a** and **b**) Wild-type control cells (left) and double knockout cells (DKO) were cultured for 6 or 24 h with the indicated concentrations of LTX-401, followed by double-staining with DAPI together with $DiOC_6(3)$ and cytofluorometric detection of dead cells ($DAPI^+$) and dying cells ($DAPI^+$ $DiOC_6(3)$low). Results are shown for pairs of WT and *Bax*; *Bak* DKO mouse embryonic fibroblasts (MEF) (**a**) and WT and *BAX*; *BAK* DKO HCT116 cells (**b**). Columns indicate means ± S.D. of triplicates. Asterisks indicate significant (unpaired Student's *t*-test) changes with respect to untreated controls (Ctr). $^*P<0.05$; $^{**}P<0.01$; $^{***}P<0.001$. (**c**) *Bax*; *Bak* WT and DKO MEF were treated with either 12.5 μg/ml LTX-315 or 6.25 μg/ml LTX-401 and the trans-Golgi protein GALT1 was stained by immunofluorescence in quadruplicate assessments. No significant change between the clonal cell lines was detected with regard to Golgi fragmentation. (**d** and **e**) The removal of mitochondria from U2OS cells stably expressing a mCherry-Parkin fusion protein was achieved by treatment with 10 μM CCCP for 48 h. The decrease in fluorescence intensity of mitochondria-specific TOMM20 signal upon immunofluorescence detection was taken as an indication for mitochondria depletion (**d**). The statistical evaluation is shown in (**e**). (**f**) U2OS cells expressing mCherry-Parkin upon continuous treatment with either 100 μM CCCP for 30 min (to depolarize mitochondria) or 10 μM for 48 h (to deplete mitochondria). Subsequently, the cells were treated with the indicated concentrations of LTX-401 for additional 6 or 24 h. Following the cells were subjected to microscopic analysis and the percent of cells that depict necrotic ($DAPI^+$) phenotypes are shown. Representative images of U2OS cells depleted or not from mitochondria were stained for the trans-Golgi marker GALT1 by immunofluorescence. Asterisks indicate significant differences (unpaired Student's *t*-test) with respect to PBS-treated controls. $^*P<0.05$; $^{**}P<0.01$; $^{***}P<0.001$

Subcellular fractionation. 10×10^3 U2OS cells were seeded per condition in 145 mm cellstar culture dishes (Greiner Bio-One) and allowed to adapt for 24 h. Thereafter the cells were treated as indicated and incubated for additional 6 h before being harvested. Therefore, the cells were rinsed with ice cold PBS (pH 7.4) and 3 dishes per condition were collected with a cell scraper in harvesting buffer (PBS, pH 7.4; 1 mM HEPES; 1 mM EDTA). Golgi was enriched using the Golgi isolation kit from Sigma Aldrich. In short: Cells were washed once and the pellet was resuspended in harvesting buffer, subjected to 10 min incubation on ice, and subsequently grinded 100 times on ice using a dounce homogenizer and centrifuged at 700 × *g* for 10 min. The supernatant was recovered and centrifuged at 10 000 × g for 30 min to obtain the cytosolic fraction (from the supernatant). The pellet was further washed with ice cold PBS and centrifuged 5 min at 450 × *g*. After centrifugation, the pellet was resuspended in 1 ml of cold isolation buffer B (75 mM sucrose; 20 mM Hepes; 225 mM mannitol; 0.5 mM EDTA, pH 7.2), placed on ice and grinded 100 times using a dounce homogenizer and following centrifuged at 750 × *g* for 20 min. The supernatant was re-centrifuged at 10 000 × *g* for 10 min to obtain the mitochondrial fraction. The purity of the fractions was analyzed by immunobloting. For detection by mass spectrometry the supernatant of the cytosolic fraction was centrifuged at 10 000 × *g* for 1 min at 4 °C and 40 μl of supernatant were mixed with 2 μl of formic acid (Sigma Aldrich). The pellet of the mitochondrial fraction was solubilized in 100 μl of water and 40 μl of solution were mixed with 2 μl of formic acid (Sigma Aldrich).

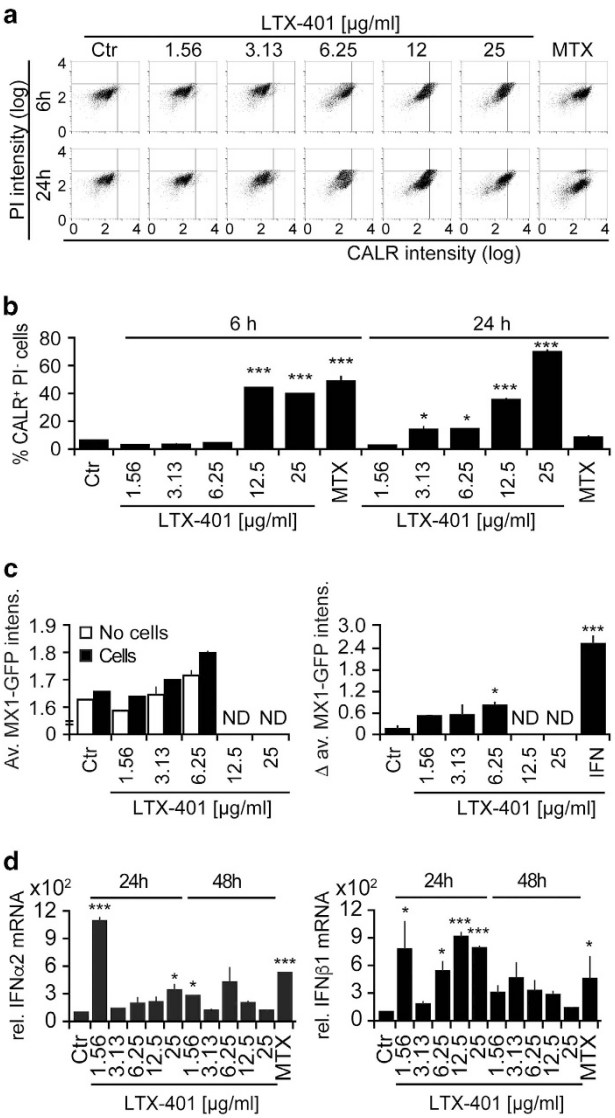

Figure 7 Induction of ICD hallmarks by LTX-401. (**a** and **b**) U2OS cells were treated for the indicated period (6 or 24 h) with LTX-401, mitoxantrone (MTX) or carbonyl cyanide *m*-chlorophenyl hydrazine (CCCP). Cells were analyzed for CALR exposure by surface immunofluorescence staining in viable, DAPI-negative cells (representative cytofluorometry scatterplots in (**a**), statistical analyses in (**b**)). Asterisks indicate significant differences (unpaired Student's *t*-test) with respect to untreated controls. *$P<0.05$; **$P<0.01$; ***$P<0.001$. (**c** and **d**) LTX-401 was added at variable concentrations to culture media (white bars) or U2OS cell cultures (black bars). Recombinant IFN-α1 was used as a positive control. After 24 h the culture supernatants were recovered and added to fresh cultures (1 : 16 dilution) of U2OS cells stably expressing green fluorescent protein (GFP) under the MX1 promoter (MX1-GFP). After an additional 48 h culture period, cells were fixed, counterstained with Hoechst 33342 and subjected to automated fluorescence microscopy and image analysis. Representative raw data of quantitation (means ± S.D. of triplicates) and the subtraction of replicate experiments of initially cell-free *versus* cell-containing cultures in (**c**). (**d**) Detection of type-1 interferons by RT-PCR. Cells were incubated as indicated with variable amounts of LTX-401 for distinct periods and then subjected to mRNA extraction and RT-PCR. Asterisks indicate significant differences (unpaired Student's *t*-test) with respect to untreated controls. *$P<0.05$; **$P<0.01$; ***$P<0.001$

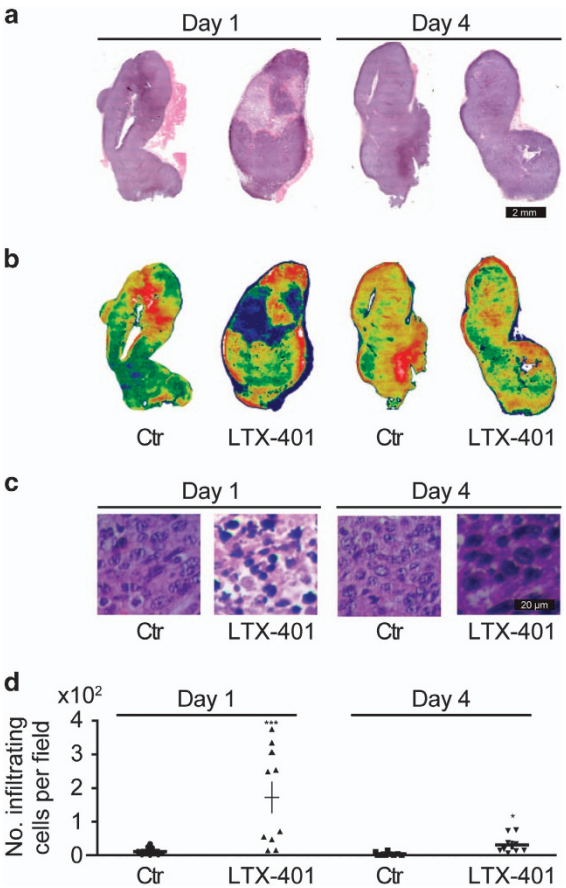

Figure 8 Macroscopic and microscopic signs of immune infiltrate in LTX-401-induced necrotic lesions *in vivo*. MCA205 fibrosarcoma was established on C57/Bl6 mice and injected with PBS (control, Ctr) or LTX-401. Tumors were harvested at day 1 or 4 later and were photographed after excision to document their macroscopic appearance (**a**) and subjected to hematoxilin and eosin (HE) staining (raw appearance in (**a**), ratio of eosin over hematoxilin in (**b**)). Representative HE staining patterns of necrotic areas are shown in (**c**) and the number of infiltrating leukocytes per view field was determined in (**d**). Asterisks indicate significant differences (unpaired Student's *t*-test) with respect to PBS-treated controls. *$P<0.05$; **$P<0.01$; ***$P<0.001$

Immunoblotting. Immunoblotting was performed following standard procedures. In short, 10 μg of protein were separated on NuPAGE Novex Bis-Tris 4–12% pre-cast gels (Invitrogen-Life Technologies, Carlsbad, CA, USA) and transferred to Immobilon polyvinylidene difluoride membranes (Merck-Millipore, Darmstadt, Germany). Unspecific binding was reduced by incubating the membranes for 1 h in 0.05% Tween 20 (v/v in TBS) supplemented with 5% w/v bovine serum albumin (Euromedex, Souffelweyersheim, France). Following, membranes were probed with antibodies specific for GALT1 and TOMM20 (Abcam). Primary antibodies were revealed with species-specific immunoglobulin G conjugated to horseradish peroxidase (Southern Biotech, Birmingham, AL, USA), followed by chemiluminescence analysis with the SuperSignal West Pico reagent by means of an ImageQuant 4000 (GE Healthcare, Little Chalfont, UK).

Targeted analysis of intracellular metabolites by UHPLC coupled to a Triple Quadrupole (QQQ) mass spectrometer. Targeted analysis was performed on a RRLC 1260 system (Agilent Technologies, Waldbronn, Germany) coupled to a Triple Quadrupole 6410 (Agilent Technologies) equipped with an electrospray source operating in positive mode. The capillary voltage was set to 4.5 kV and the gas temperature to 350 °C, using a gas flow of 12 l/min. Five microliters of sample were injected on a Zorbax Eclipse plus C18 column (100 mm × 2.1 mm, particle size 1.8 μm) from Agilent technologies and heated at 40 °C. The mobile phase consisted of water 0.2% acetic acid (A) and acetonitrile (B), with a flow rate set to 0.3 ml/min and initial 90% phase A and 10% phase B. The gradient changed as follows: initial conditions were maintained during 1.4 min. Molecules were then eluted using a gradient from 10 to 95% phase B over 0.6 min. The column was washed using 95% mobile phase B for 2.5 min and equilibrated using 10% mobile phase B for 2.75 min. The needle was rinsed with 50% acetonitrile in water (v/v). The autosampler was kept at 4 °C.

MRM transitions were as follows (all in positive mode):

Compound name	Precursor ion (*m/z*)	Product ion (*m/z*)	Fragmentor (V)	Collision energy (V)
LTX-315 Target	360,7	129,1	70	20
LTX-315 Qualifier	360,7	443,3	70	15
LTX-315 Qualifier	360,7	629,4	70	15
LTX-315 Qualifier	360,7	757,4	70	10
LTX-401 Target	368.3	377.3	70	22
LTX-401 Qualifier	368.3	173.3	70	22

Data processing and statistical analyses. Unless otherwise specified, experiments were performed in triplicate parallel instances and repeated at least once, and data were analyzed with the R software (http://www.r-project.org/). Microscopy images were segmented and analyzed by means of the MetaXpress (Molecular Devices) software and numerical data were further processed with R. Unless otherwise specified, data are presented as means ± S.D. Significances have been evaluated using an unpaired Welch's *t*-test to rectify possible differences in sample variances. Thresholds for the minimum number of events in each analysis necessary to apply further statistics were calculated based on a medium effect size (according to Cohen's conventional criteria) using the pwr package for R with a targeted value of 0.95. Samples that did not match the requirements were marked ND and were excluded from the analysis.

Cell death assays. 5×10^3 human MEF or HCT116 cells were seeded in 96-well cell culture plates and allowed to adapt for 24 h, then maintained in control conditions or exposed to LTX-315 or -401 for 6 or 24 h. For flow cytometry, culture supernatants were transferred to V-shaped 96-well plates and cells were detached with 30 μl TrypsinLE Express per well, then resuspended in 30 μl of medium and joined with the supernatant. The cells were centrifuged 5 min at 200 × *g* and the pellet was resuspended in medium supplemented with 40 nM $DiOC_6(3)$ and 2 μM DAPI (all from Molecular Probes-Life Technologies, Carlsbad, CA, USA) and incubated for 30 min at 37 °C before acquisition. Cytofluorometric acquisition was performed on a Cyan ADP (Beckman Coulter).

Mitophagy induction. U2OS cells stably expressing PARKIN-mCherry were treated with 10 μM of CCCP for 48 h for the induction of mitophagy. Following the depletion of mitochondria cells were washed and treated with LTX-401 for additional 6 or 24 h. Decreased mitochondrial content was verified by mitochondria-specific anti-TOMM20 immunostaining.

Immunostaining. 5×10^3 U2OS cells were seeded into black 96-well nuclear imaging plates (Greiner Bio-One) and allowed to adapt for 24 h. Thereafter the cells were treated with Lytix-401 and indicated controls and incubated for additional 6 or 24 h before fixation in 3.7% (w/v) paraformaldehyde in PBS supplemented with 1 μM Hoechst 33342 for 20 min at room temperature (RT). Following cells were permeabilized using 0.1% Triton in PBS for 10 min at RT. Unspecific binding was minimized by incubating the cell in 2% BSA in PBS for 10 min at RT followed by incubation with the primary antibody diluted in 2% BSA in PBS agitated over night at 4 °C. The cells were rinsed twice with 2% BSA in PBS and further incubated with AlexaFluor-coupled secondary antibodies for 1 h at RT, rinsed again twice with PBS and subjected to imaging using an ImageXpress micro XL automated bioimager (Molecular Devices) equipped with a PlanApo 20X/0.75 NA objective (Nikon). For some of the assays cells were additionally stained with 200 nM MitoTracker green before imaging.

Tissue staining and imaging. Tumors were fixed upon dissection at day 1 and day 4 after treatment with 3.7% of PFA for 4 h at ambient temperature. Following the tissue was incubated in 30% sucrose solution for 24 h at 4 °C. The tumor was used for HE staining according to standard procedures, mounted on coverslips and imaged using an automated Microvision slide scanner (Olympus, Tokyo, Japan). The percentage of phenotypically altered cells was evaluated using imageJ (http://imagej.nih.gov/ij/).

Determination of surface exposed CALR by immunofluorescence. Cells were collected and rinsed twice with cold PBS. Following the cells were incubated with an anti-CALR antibody (ab2907; Abcam) diluted in cold blocking buffer (1% BSA in PBS) for 60 min on ice, followed by washing and incubation with AlexaFluor 488-conjugates (Invitrogen) in blocking buffer (for 30 min). Thereafter cells were washed in cold PBS, the vital dye PI was added to a final concentration of 1 μg/ml, and samples were analyzed by means of a CyAn ADP (Beckman Coulter) coupled to a Hypercite autosampler (IntelliCyte, Albuquerque, NM, USA). The analysis was limited to living (PI^-) cells. Data were statistically evaluated using R (https://www.r-project.org).

Assessment of ATP secretion. For the detection of ATP-containing vesicles, the cells were labeled with quinacrine as described.[12] In short, cells were incubated with 5 μM quinacrine and 1 μg/ml Hoechst 33342 in Krebs-Ringer solution (125 mM NaCl, 5 mM KCl, 1 mM $MgSO_4$, 0.7 mM KH_2PO_4, 2 mM $CaCl_2$, 6 mM glucose and 25 mM Hepes, pH 7.4) for 30 min at 37 °C. Thereafter, cells were rinsed with Krebs-Ringer and living cells were microscopically examined. Alternatively the concentration of extracellular ATP was assessed by means of the ENLITEN ATP assay (Promega, Madison, WI, USA), based on luciferin conversion, following the manufacturer's instructions. Chemoluminescence was measured using an i3 Paradigm multi-label reader (Molecular Devices).

Determination of extracellular HMGB1 concentration. Quantification of HMGB1 in cell supernatants was performed by means of an enzyme-linked immunosorbent assay (HMGB1 ELISA kit II; Shino Test Corporation, Tokyo, Japan) following the manufacturer's instructions. Absorbance was analyzed by means of an i3 Paradigm multi-label reader (Molecular Devices).

Quantitative real-time PCR for interferon production. RNA was extracted and genomic DNA was removed using the GeneJet RNA purification kit (ThermoScientific, Waltham, MA, USA) following the manufacturer's instructions. Five micrograms of total RNA from each sample was reverse-transcribed into cDNA with the Maxima first strand cDNA synthesis kit (ThermoScientific) using random primers and deoxynucleoside triphosphate (Invitrogen). The specific expression level of IFN-related genes was analyzed by means of the Power SYBR Green PCR Master Mix (ThermoScientific) containing primers (Invitrogen) by means of a StepOnePlus Real-Time PCR System (ThermoScientific). qRT-PCR data were normalized to the expression levels of the housekeeping gene HPRT1.

Mouse experiments. Female wild-type C57Bl/6 mice at the age of 6–7 weeks were obtained from Harlan France (Gannat, France) and maintained in the animal facility at Gustave Roussy Campus Cancer in specific pathogen-free conditions in a temperature-controlled environment with 12 h light, 12 h dark cycles and received food and water *ad libitum*. Animal experiments were in compliance with the EU Directive 63/2010 and protocols 2013_094A were approved by the Ethical Committee of the Gustave Roussy Campus Cancer (CEEA IRCIV/IGR no. 26,

registered at the French Ministry of Research). MCA205 tumors were established in C57Bl/6 hosts by subcutaneously inoculating 500 000 cells. When tumors became palpable, 300 μg of LTX-401 was injected intratumorally. One and four days later tumors were recovered.

Conflict of Interest

The authors declare no conflict of interest.

Acknowledgements. HCT116 BAX BAK DKO were a generous gift from Dr. Bert Vogelstein. HZ and PL are supported by the China Scholarship Council, LZ is supported by the Ligue contre le Cancer, GK and LZ are supported by the Ligue contre le Cancer (équipes labelisées); Agence National de la Recherche (ANR)—Projets blancs; ANR under the frame of E-Rare-2, the ERA-Net for Research on Rare Diseases; Association pour la recherche sur le cancer (ARC); Cancéropôle Ile-de-France; Institut National du Cancer (INCa); Fondation Bettencourt-Schueller; Fondation de France; Fondation pour la Recherche Médicale (FRM); the European Commission (ArtForce); the European Research Council (ERC); the LabEx Immuno-Oncology; the SIRIC Stratified Oncology Cell DNA Repair and Tumor Immune Elimination (SOCRATE); the SIRIC Cancer Research and Personalized Medicine (CARPEM); the Swiss Bridge Foundation, ISREC and the Paris Alliance of Cancer Research Institutes (PACRI). This project was supported by Lytix Biopharma Ltd.

1. Ausbacher D, Svineng G, Hansen T, Strom MB. Anticancer mechanisms of action of two small amphipathic beta(2,2)-amino acid derivatives derived from antimicrobial peptides. *Biochim Biophys Acta* 2012; **1818**: 2917–2925.
2. Eike LM, Mauseth B, Camilio KA, Rekdal O, Sveinbjornsson B. The Cytolytic amphipathic beta(2,2)-amino acid LTX-401 induces DAMP release in melanoma cells and causes complete regression of B16 melanoma. *PLoS One* 2016; **11**: e0148980.
3. Camilio KA, Rekdal O, Sveinbjornsson B. LTX-315 (Oncopore): a short synthetic anticancer peptide and novel immunotherapeutic agent. *Oncoimmunology* 2014; **3**: e29181.
4. Forveille S, Zhou H, Sauvat A, Bezu L, Muller K, Liu P *et al.* The oncolytic peptide LTX-315 triggers necrotic cell death. *Cell Cycle* 2015; **14**: 3506–3512.
5. Zhou H, Forveille S, Sauvat A, Yamazaki T, Senovilla L, Ma Y *et al.* The oncolytic peptide LTX-315 triggers immunogenic cell death. *Cell Death Dis* 2016; **7**: e2134.
6. Yamazaki T, Pitt JM, Vetizou M, Marabelle A, Flores C, Rekdal O *et al.* The oncolytic peptide LTX-315 overcomes resistance of cancers to immunotherapy with CTLA4 checkpoint blockade. *Cell Death Differ* 2016; **23**: 1004–1015.
7. Camilio KA, Berge G, Ravuri CS, Rekdal O, Sveinbjornsson B. Complete regression and systemic protective immune responses obtained in B16 melanomas after treatment with LTX-315. *Cancer Immunol Immunother* 2014; **63**: 601–613.
8. Zhou H, Forveille S, Sauvat A, Sica V, Izzo V, Durand S *et al.* The oncolytic peptide LTX-315 kills cancer cells through Bax/Bak-regulated mitochondrial membrane permeabilization. *Oncotarget* 2015; **6**: 26599–26614.
9. Kroemer G, Galluzzi L, Kepp O, Zitvogel L. Immunogenic cell death in cancer therapy. *Annu Rev Immunol* 2013; **31**: 51–72.
10. Eike LM, Yang N, Rekdal O, Sveinbjornsson B. The oncolytic peptide LTX-315 induces cell death and DAMP release by mitochondria distortion in human melanoma cells. *Oncotarget* 2015; **6**: 34910–34923.
11. Pelham HR. Multiple targets for brefeldin A. *Cell* 1991; **67**: 449–451.
12. Verhagen AM, Ekert PG, Pakusch M, Silke J, Connolly LM, Reid GE *et al.* Identification of DIABLO, a mammalian protein that promotes apoptosis by binding to and antagonizing IAP proteins. *Cell* 2000; **102**: 43–53.
13. Wei MC, Zong WX, Cheng EH, Lindsten T, Panoutsakopoulou V, Ross AJ *et al.* Proapoptotic BAX and BAK: a requisite gateway to mitochondrial dysfunction and death. *Science* 2001; **292**: 727–730.
14. Narendra D, Tanaka A, Suen DF, Youle RJ. Parkin is recruited selectively to impaired mitochondria and promotes their autophagy. *J Cell Biol* 2008; **183**: 795–803.
15. Zhang L, Yu J, Park BH, Kinzler KW, Vogelstein B. Role of BAX in the apoptotic response to anticancer agents. *Science* 2000; **290**: 989–992.
16. Galluzzi L, Aaronson SA, Abrams J, Alnemri ES, Andrews DW, Baehrecke EH *et al.* Guidelines for the use and interpretation of assays for monitoring cell death in higher eukaryotes. *Cell Death Differ* 2009; **16**: 1093–1107.
17. Niso-Santano M, Bravo-San Pedro JM, Maiuri MC, Tavernarakis N, Cecconi F, Madeo F *et al.* Novel inducers of BECN1-independent autophagy: cis-unsaturated fatty acids. *Autophagy* 2015; **11**: 575–577.
18. Niso-Santano M, Malik SA, Pietrocola F, Bravo-San Pedro JM, Marino G, Cianfanelli V *et al.* Unsaturated fatty acids induce non-canonical autophagy. *EMBO J* 2015; **34**: 1025–1041.
19. Cheng JP, Betin VM, Weir H, Shelmani GM, Moss DK, Lane JD. Caspase cleavage of the Golgi stacking factor GRASP65 is required for Fas/CD95-mediated apoptosis. *Cell Death Dis* 2010; **1**: e82.
20. Dumitru R, Gama V, Fagan BM, Bower JJ, Swahari V, Pevny LH *et al.* Human embryonic stem cells have constitutively active Bax at the Golgi and are primed to undergo rapid apoptosis. *Mol Cell* 2012; **46**: 573–583.
21. Tu S, McStay GP, Boucher LM, Mak T, Beere HM, Green DR. In situ trapping of activated initiator caspases reveals a role for caspase-2 in heat shock-induced apoptosis. *Nat Cell Biol* 2006; **8**: 72–77.
22. Galluzzi L, Bravo-San Pedro JM, Kroemer G. Organelle-specific initiation of cell death. *Nat Cell Biol* 2014; **16**: 728–736.
23. Galluzzi L, Kepp O, Krautwald S, Kroemer G, Linkermann A. Molecular mechanisms of regulated necrosis. *Semin Cell Dev Biol* 2014; **35**: 24–32.
24. Galluzzi L, Bravo-San Pedro JM, Vitale I, Aaronson SA, Abrams JM, Adam D *et al.* Essential versus accessory aspects of cell death: recommendations of the NCCD 2015. *Cell Death Differ 2015* **22**: 58–73.
25. Martins I, Kepp O, Schlemmer F, Adjemian S, Tailler M, Shen S *et al.* Restoration of the immunogenicity of cisplatin-induced cancer cell death by endoplasmic reticulum stress. *Oncogene* 2011; **30**: 1147–1158.

Supplementary Information accompanies this paper on Cell Death and Differentiation website (http://www.nature.com/cdd)